Tunable lateral displacement and spin beam splitter for ballistic electrons in two-dimensional magnetic-electric nanostructures

Xi Chen,[1,*] Chun-Fang Li,[1,2,†] and Yue Ban[1]
[1]*Department of Physics, Shanghai University, Shanghai 200444, People's Republic of China*
[2]*State Key Laboratory of Transient Optics and Photonics, Xi'an Institute of Optics and Precision Mechanics, CAS, Xi'an 710119, People's Republic of China*
(Received 13 December 2007; published 20 February 2008)

We investigate the lateral displacements for ballistic electron beams in a two-dimensional electron gas modulated by metallic ferromagnetic (FM) stripes with parallel and antiparallel (AP) magnetization configurations. It is shown that the displacements are negative as well as positive, which can be controlled by adjusting the electric potential induced by the applied voltage and the magnetic field strength of FM stripes. Based on these phenomena, we propose an efficient way to realize a spin beam splitter, which can completely separate spin-up and spin-down electron beams in the AP configuration by their corresponding spatial positions.

DOI: 10.1103/PhysRevB.77.073307 PACS number(s): 73.63.−b, 73.23.Ad, 73.40.Gk, 75.75.+a

It is well established that ballistic electrons in the two-dimensional electron gas (2DEG) are reflected, focused, diffracted, and interfered in a manner similar to the electromagnetic waves in dielectrics,[1,2] which results from the quantum-mechanical wave nature of electrons thus have given rise to a field of research which is best described as ballistic electron optics in 2DEG systems. In the past two decades, many electronic analogs of optical devices[3,4] have been studied, including electron gratings, electron waveguide, electron interferometer, and electron wave beam splitter.

Recently, electron spin beam splitter and spin filter in different 2DEG systems have been more attractive[5–10] for the nascent field called "spintronics,"[11] which is a multidisciplinary field whose central subject is the active control and manipulation of spin degree of freedom in solid systems. For example, Khodas *et al.*[8] have proposed the basic schemes for filtration and control of the electron spin by electron spin optics in the 2DEG structures with the Rashba–Dresselhaus spin-orbit coupling. Moreover, spin beam splitters or spatially separating spin filters have also been investigated by other opticslike phenomena, respectively, such as spin double refraction[9] and negative refraction.[10] However, considering some disadvantages of the 2DEG structures with spin-orbit coupling, Frustaglia *et al.*[12] have studied spin filters by pure quantum interference effect. Dragoman[13] has lately presented an alternative spin beam splitter in 2DEG systems, in terms of magnetic depopulation of subbands in magnetic fields.

In this Brief Report, we will investigate the lateral displacements for ballistic electron beams in a 2DEG modulated by metallic ferromagnetic (FM) stripes with parallel (P) and antiparallel (AP) magnetization configurations. The displacements can be negative and positive, which can be controlled by adjusting the total electric potential and the magnetic field strength of FM stripes. More interestingly, we propose a spin beam splitter as a potential application of an intriguing phenomenon in which large and opposite lateral displacements may occur simultaneously for spin-down and spin-up electron beams in the AP configurations. As a matter of fact, the displacements are closely related to the Goos–Hänchen (GH) effect in optics[14] and are the electronic analogous to the simultaneously large and opposite generalized GH shifts for TE and TM light beams in an asymmetric double-prism configuration.[15] Thus, the tunable negative or positive displacement introduced here provides a completely different mechanism of spin-polarized electron splitting also at the nanoscale level but with more design flexibility.

The system under consideration is a magnetically modulated 2DEG formed usually in a modulation-doped semiconductor heterostructure,[16] which can be experimentally realized by depositing two metallic FM stripes on top and bottom of the semiconductor heterostructure, as schematically depicted in Fig. 1(a). For the small distances between 2DEG and FM stripes, the magnetic field provided by two FM stripes is approximated[17] as $B_z(x)=[B_1\delta(x+a/2)-\chi B_2\delta(x-a/2)]$, and the total electric potential induced by the negative voltage applied directly to the 2DEG, $U(x)=U\Theta(a/2-|x|)$, is homogenous in the y di-

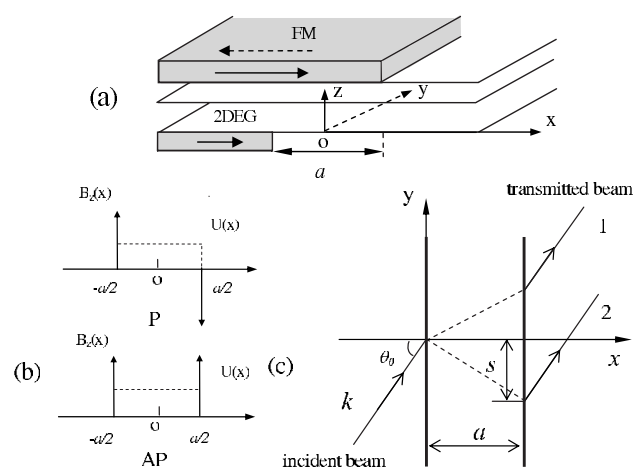

FIG. 1. (a) Schematic illustration of the magnetic-electric nanostructure with two metallic FM stripes deposited on top and bottom of the semiconductor heterostructure. (b) The magnetic-electric barrier models exploited here correspond to the P and AP magnetization configurations of two FM stripes, respectively. (c) The (1) positive and (2) negative lateral displacements of ballistic electron beams in this structure.

 ©2008 The American Physical Society

rection and varies only along the x axis,[18] which is shown in Fig. 1(b), where χ represents the P and AP magnetization configurations of two FM stripes ($\chi=+1$ for P and $\chi=-1$ for AP). The Hamiltonian describing such a system in the (x,y) plane, within the single particle effective mass approximation, is

$$H=\frac{p_x^2}{2m^*}+\frac{[p_y+e\mathbf{A}_y(x)]^2}{2m^*}+U(x)+\frac{eg^*}{2m_0}\frac{\sigma\hbar}{2}B_z(x), \quad (1)$$

where m^* is the electron effective mass and m_0 is the free electron mass, (p_x,p_y) are the components of the electron momentum, g^* is the effective Landé factor of electron, $\sigma=+1/-1$ for spin-up/spin-down electrons, and $\mathbf{A}_y(x)$ is the y-component of the vector potential given, in Landau gauge, by $\vec{\mathbf{A}}=[0,\mathbf{A}_y(x),0]$. We express all the relevant quantities in dimensionless form: (1) the magnetic field $B_z(x)\to B_0B_z(x)$, (2) the vector potential $\mathbf{A}(x)\to B_0l_B\mathbf{A}(x)$, (3) the coordinates $\mathbf{r}\to l_B\mathbf{r}$, and (4) the energy $E\to E\hbar\omega_c$, where $\omega_c=eB_0/m^*$ is the cyclotron frequency and $l_B=\sqrt{\hbar/eB_0}$ is the magnetic length with B_0 as some typical magnetic field. For GaAs and an estimated $B_0=0.1$ T, we have $l_B=813$ nm, $\hbar\omega_c=0.17$ meV, $g^*=0.44$, and $m^*=0.067m_0$.

A two-dimensional electron beam of incidence energy E comes from the left with an incidence angle θ_0 in (x,y) plane, as is depicted in Fig. 1(c). Let $\Psi_i(\vec{x})=A(k_y)\exp\{i[k_x^l(x+a/2)+k_yy]\}$ be the plane wave component of the incident beam, where $k^l=\sqrt{2E}$, $k_y=k^l\sin\theta$, $k_x^l=k^l\cos\theta$, θ stands for the incidence angle of the contributed plane wave, and $A(k_y)$ is the angular-spectrum distribution. Because the system is translationally invariant along the y direction, the solution of the stationary Schrödinger equation $H\Psi(x,y)=E\Psi(x,y)$ can be written as $\Psi(x,y)=\psi(x)\exp(ik_yy)$. The wave function $\psi(x)$ satisfies the following one-dimensional Schrödinger equation:

$$\left\{\frac{d^2}{dx^2}-2[E-U_{\text{eff}}(x,k_y,\sigma)]\right\}\psi(x)=0, \quad (2)$$

where the effective potential in the barrier region $U_{eff}(x,k_y,\sigma)=U+[k_y+A_y(x)]^2/2+m^*g^*\sigma B_z(x)/4m_0$ depends not only on the wave vector k_y but also on the interaction between the electron spin and the nonhomogeneous magnetic field. According to Eq. (2) and boundary conditions, that is, the continuity of the wave functions and their derivations at the boundaries, the wave function of the corresponding plane wave of transmitted beam is found to be $\Psi_t(\vec{x})=t(k_y)A(k_y)\exp\{i[k_x^r(x-a/2)+k_yy]\}$, and the amplitude transmission coefficient $t(k_y)=e^{i\phi}/g$ is determined by the following complex number: $ge^{i\phi}=2k_x^rk_x'/(M+iN)$, where

$$M=k_x'(k_x^l+k_x^r)+\frac{m^*g\sigma}{2m_0}(k_x^lB_2-\chi k_x^rB_1)\tan k_x'a, \quad (3)$$

$$N=-\frac{m^*g\sigma}{2m_0}(B_1-\chi B_2)k_x'+\left[k_x^lk_x^r+k'^2+\left(\frac{m^*g\sigma}{2m_0}\right)^2(\chi B_1B_2)\right]\tan k_x'a, \quad (4)$$

so that the total phase shift of the transmitted beam at $x=a/2$ with respect to the incident one at $x=-a/2$ is

$$\tan\phi\equiv\frac{N}{M},$$

where $k_x'=[2E-(k_y+B_1)^2]^{1/2}$ and $k_x^r=[2E-(k_y+B_1-\chi B_2)^2]^{1/2}$. As indicated in Fig. 1(c), the lateral displacement of the transmitted beam is defined, according to the stationary-phase approximation,[2,19,20] as

$$s=-d\phi/dk_{y0}, \quad (5)$$

where the subscript 0 in this Brief Report denotes the values taken at $k_y=k_{y0}$, namely, $\theta=\theta_0$. It is clearly seen from Eqs. (3) and (4) that the lateral displacement presented here is dependent on the electron spin, except only when $B_1=B_2$ in the P case of $\chi=1$. For the simplicity, we will let $B_1=B_2=B$ in the following discussions on the lateral displacement in the P and AP configurations, respectively.

First, the lateral displacement [Eq. (5)] in the P case is reduced to

$$s=\frac{s_g}{2g_0^2}\left\{\left(\frac{k_{x0}}{k_{x0}'}+\frac{k_{x0}'}{k_{x0}}+\frac{k_0^2}{k_{x0}k_{x0}'}\right)-\left[\left(1-\frac{k_{x0}'^2}{k_{x0}^2}\right)\left(\frac{k_{x0}}{k_{x0}'}-\frac{k_{x0}'}{k_{x0}}\frac{k_{y0}}{k_{y0}'}\right)+\frac{k_0^2}{k_{x0}^2}\left(\frac{k_{x0}}{k_{x0}'}+\frac{k_{x0}'}{k_{x0}}\frac{k_{y0}}{k_{y0}'}\right)\right]\frac{\sin 2k_{x0}'a}{2k_{x0}'a}\right\}, \quad (6)$$

where $k_{x0}=(2E-k_{y0}^2)^{1/2}$, $k_0=m^*g\sigma B/2m_0$, $k_{y0}'=k_{y0}+B$, $s_g=a\tan\theta_0'$, $\tan\theta_0'=k_{y0}'/k_{x0}'$, and the transmission probability $1/g_0^2=T_0$ is closely related to the measurable ballistic conductance G, according to the well-known Landauer–Büttiker formula.[21]

Equation (6) indicates that the modulation of the lateral displacement s relies on the following properties. (1) When transmission resonances occur, that is to say, when $k_{x0}'a=m\pi$ $(m=1,2,3,\ldots)$ is satisfied, $T_0=1$. At resonances, the lateral displacement is also maximal,

$$s_{max}\equiv s|_{k_{x0}'a=m\pi}=\frac{s_g}{2}\left(\frac{k_{x0}}{k_{x0}'}+\frac{k_{x0}'}{k_{x0}}+\frac{k_0^2}{k_{x0}k_{x0}'}\right).$$

The resonance condition depends on the electric potential U and magnetic field strength B. (2) The lateral displacement can be negative under the necessary condition, which can be expressed as a restriction to the incidence angle θ_0 as follows,

$$\cos\theta_0<\left[\frac{-U-(B^2-k_0^2)/2}{2E}\right]^{1/2}\equiv\cos\theta_t, \quad (7)$$

because of the factor $\sin 2k_{x0}'a/2k_{x0}'a\leq 1$. This shows that if the incidence angle satisfies the condition [Eq. (7)], that is to say, if θ_0 is larger than the threshold angle θ_t, one can always find a width a where the displacement is negative. Indeed,

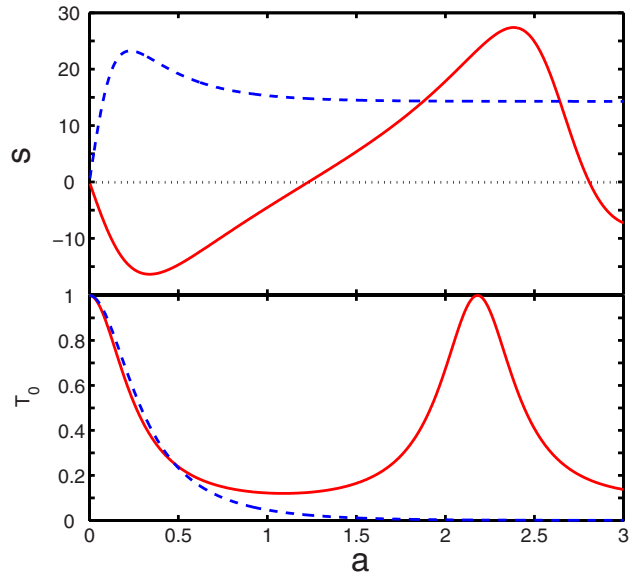

FIG. 2. (Color online) Dependence of the displacements and the corresponding transmission probabilities on the width a for $U=1$ (solid curve) and $U=-1$ (dashed curve), respectively, where $E=5$, $B=0.1$, and $\theta_0=85°$.

Eq. (7) is not satisfied by any incidence angle if $U>0$, since $B^2>k_0^2$. That means that the displacement is always positive for $U>0$, while it can be negative for $U<0$. The lateral displacement can thus be easily tuned from positive to negative by adjusting the electric potential U, with changing the corresponding negative and positive voltages applied directly to 2DEG.

Further investigations show that Eq. (6) is still valid in the evanescent case of $2(E-U)<(k_y+B)^2$, only if k_x' is replaced by $i\kappa$, where $\kappa=[(k_y+B)^2-2(E-U)]^{1/2}$. The displacement in this case saturates to a positive constant in the opaque limit $a\gg 1/\kappa_0$ with the transmission probability decaying exponentially in the same ways as that in the semiconductor barrier structure.[20]

Figure 2 shows the typical dependence of the lateral displacement [Eq. (6)] and the corresponding transmission probability on the width a for $U=1$ (dash curve) and $U=-1$ (solid curve), respectively, where $E=5$, $B=0.1$, and $\theta_0=85°$ ($\theta_t=71.5°$), namely, $k_{y0}=3.2$. The displacement and transmission probability are identical for spin-up and spin-down electrons in this case. It is also shown that the displacement depends periodically on the width a in the propagating case, while it saturates to a constant for an opaque barrier in the evanescent case. Calculations under those conditions show that the displacements for $U=-1$ and $U=1$ are approximately equal to -12.48 and 22.36 for $a=0.5$, respectively. This implies that the lateral displacements can be opposite for the different signs of U with the approximately equal amplitude of the corresponding transmission probabilities.

Figure 3 presents the modulation of the lateral displacements by the magnetic field strength B at the fixed electric potential U. From these four curves, one can observe the absorbing feature that the displacements can be changed from negative to positive with the increasing U. Another observation from Fig. 3 is that, with the increasing B, the curve of lateral displacement shifts leftward. Moreover, when U and B are large enough, the lateral displacements always tend to positive values in the evanescent case. All those features result from the dependence of the effective potential U_{eff} on U and B. This leads to the modulations of the displacement by the total electric potential induced by the voltage applied directly to 2DEG and magnetic field strength produced by FM stripes.

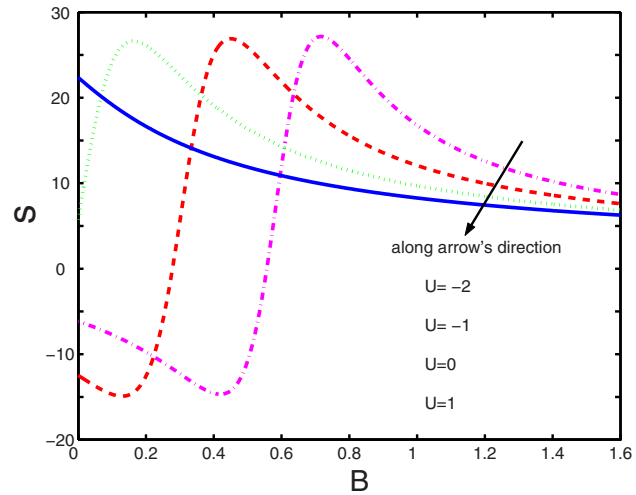

FIG. 3. (Color online) Modulation of the displacements by the magnetic field strength B at different fixed electric potentials $U=-2$ (dotted-dashed curve), -1 (dashed curve), 0 (dotted curve), and 1 (solid curve), respectively, where $a=0.5$ and other parameters are the same as in Fig. 2.

Now, we are ready to investigate the a spin-polarized ballistic electron beam splitter based on the properties of the lateral displacements discussed above. In the AP configuration, the lateral displacement depends on the electron spin due to its asymmetry,[22] so that the spin-polarized electron beam can be separated spatially. More interestingly, Fig. 4(a) gives an example that the displacement can be opposite for spin-up and spin-down electron beams at a large incidence angle, where $E=2$, $a=0.5$, $U=-1$, and the other parameters are the same as in Fig. 2. Figure 4(b) further demonstrates the validity of the above stationary-phase analysis by numerical simulations of the Gaussian-shaped incident beam,

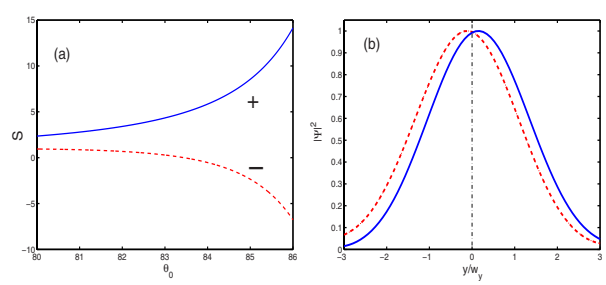

FIG. 4. (Color online) (a) Simultaneously large and opposite lateral displacements for spin-up (solid curve) and spin-down (dashed curve) electron beams, where $E=2$, $a=0.5$, $U=-1$, and the other parameters are the same as in Fig. 2. (b) Comparison of the corresponding normalized shapes of the transmitted beams.

that is to say, the transmitted beam retains well the shape of the incident beam with positive and negative displacements, within the restriction $a \ll \pi w/(2\cos\theta_0 \tan\theta_0')$,[20] where $w=10\lambda_e$. As mentioned above, the positive displacement under these physical parameters corresponds to the evanescent case, thus the displacements presented here are not large enough, which leads to the quite small spin beam split. However, further investigations show that the opposite displacements for the electron beams reflected from this system can be greatly enhanced by the transmission resonance in the same way as the generalized GH shifts for light beams in a double-prism configuration.[15] In a word, the control of the simultaneously large and opposite lateral displacements allows this system to realize the spin beam splitter, which can completely separate spin-up and spin-down electron beams in the AP configuration by their different spatial positions.

In conclusion, we have investigated theoretically and numerically the tunable lateral displacement and spin beam splitter for ballistic electrons in magnetic-electric nanostructure. The displacement presented here has the feature of GH shift, which does result from the reshaping process of the transmitted beam, because of the destructive and constructive interferences between each plane wave components undergoing the different phase shifts due to the multiple reflections in this system.[20] Recent investigations show that the lateral GH displacement and transverse displacement called Imbert–Fedorov effect relate directly to the spin Hall effect.[23] Thus, the spin-dependent displacements and related phenomena in various quantum systems, especially in the presence of spin-orbit coupling, remain as further problems. We hope that these interesting phenomena may stimulate experiments to realize novel electronic devices, such as spin filter and spin beam splitter.

This work was supported in part by the Shanghai Educational Development Foundation (2007CG52), National Natural Science Foundation of China (60377025), and the Shanghai Leading Academic Discipline Program (T0104).

*Corresponding author. xchen@shu.edu.cn
†cfli@shu.edu.cn

[1] T. K. Gaylord, E. N. Glytsis, G. N. Henderson, K. P. Martin, D. B. Walker, D. W. Wilson, and K. F. Brennan, Proc. IEEE **79**, 1159 (1991), and references therein.
[2] D. W. Wilson, E. N. Glytsis, and T. K. Gaylord, IEEE J. Quantum Electron. **29**, 1364 (1993).
[3] D. Dragoman and M. Dragoman, Prog. Quantum Electron. **23**, 131 (1999).
[4] S. Datta, *Electronic Transport in Mesoscopic Systems* (Cambridge University Press, New York, 1996), p. 276.
[5] A. A. Kiselev and K. W. Kim, Appl. Phys. Lett. **78**, 775 (2001).
[6] I. A. Shelykh, N. G. Galkin, and N. T. Bagraev, Phys. Rev. B **72**, 235316 (2005).
[7] P. Földi, O. Kálmán, M. G. Benedict, and F. M. Peeters, Phys. Rev. B **73**, 155325 (2006).
[8] M. Khodas, A. Shekhter, and A. M. Finkel'stein, Phys. Rev. Lett. **92**, 086602 (2004).
[9] V. M. Ramaglia, D. Bercioux, V. Cataudella, G. D. Filippis, and C. A. Perroni, J. Phys.: Condens. Matter **16**, 9143 (2004).
[10] X.-D. Zhang, Appl. Phys. Lett. **88**, 052114 (2006).
[11] I. Žutíc, J. Fabiam, and S. Das Sarma, Rev. Mod. Phys. **76**, 323 (2004).
[12] D. Frustaglia, M. Hentschel, and K. Richter, Phys. Rev. Lett. **87**, 256602 (2001).
[13] D. Dragoman, Physica B **367**, 92 (2005).
[14] F. Goos and H. Hänchen, Ann. Phys. **1**, 333 (1947); **5**, 251 (1949).
[15] C. F. Li and Q. Wang, Phys. Rev. E **69**, 055601(R) (2004).
[16] V. Kubrak, F. Rahman, B. L. Gallagher, P. C. Main, M. Henini, C. H. Marrows, and M. A. Howson, Appl. Phys. Lett. **74**, 2507 (1999); T. Vancura, T. Ihn, S. Broderick, K. Ensslin, W. Wegscheider, and M. Bichler, Phys. Rev. B **62**, 5074 (2000).
[17] G. Papp and F. M. Peeters, Appl. Phys. Lett. **78**, 2184 (2001); **79**, 3198 (2001); H. Z. Xu and Y. Okada, *ibid.* **79**, 3119 (2001).
[18] M.-W. Lu and G.-J. Yang, Phys. Lett. A **362**, 489 (2007); M.-W. Lu, Solid State Commun. **134**, 683 (2005).
[19] D. Bohm, *Quantum Theory* (Prentice-Hall, New York, 1951), pp. 257–261.
[20] X. Chen, C.-F. Li, and Y. Ban, Phys. Lett. A **354**, 161 (2006).
[21] M. Büttiker, Phys. Rev. Lett. **57**, 1761 (1986).
[22] F. Zhai and H. Q. Xu, Phys. Rev. Lett. **94**, 246601 (2005).
[23] M. Onoda, S. Murakami, and N. Nagaosa, Phys. Rev. Lett. **93**, 083901 (2004); N. A. Sinitsyn, Q. Niu, J. Sinova, and K. Nomura, Phys. Rev. B **72**, 045346 (2005); K. Yu. Bliokh and V. D. Freilikher, *ibid.* **74**, 174302 (2006).